ARTICLE
Journal of Cellular Biochemistry 111:49–58 (2010)

Journal of Cellular Biochemistry

Chloride Channel ClC-3 Promotion of Osteogenic Differentiation Through Runx2

Huan Wang,[1,2] Yong Mao,[3] Bin Zhang,[4] Tao Wang,[5] Feifei Li,[1] Shanmin Fu,[1] Yang Xue,[2] Ting Yang,[2] Xuan Wen,[2] Yin Ding,[1**] and Xiaohong Duan[2*]

[1]*Department of Orthodontics, School of Stomatology, Fourth Military Medical University, Xi'an 710032, China*

[2]*Department of Oral Biology, School of Stomatology, Fourth Military Medical University, Xi'an 710032, China*

[3]*Department of Prosthodontics, School of Stomatology, Fourth Military Medical University, Xi'an 710032, China*

[4]*Department of Hematopoietic Stem Cell Transplantation, Affiliated Hospital to Academy of Military Medical Sciences, No. 8, East Street, Fengtai District, Beijing 100071, People's Republic of China*

[5]*Department of Biochemistry and Molecular Biology, State Key Lab of Cancer Biology, Fourth Military Medical University, Xi'an 710032, China*

ABSTRACT

ClC-3 chloride channel has been speculated to contribute to the acidification of synaptic vesicles and endosomes. However, the biological function of ClC-3 in osteogenesis remains to be determined. In this study, we first analyzed ClC-3 expression in MC3T3-E1 cells and primary mouse osteoblasts and then performed the osteoinductive procedure to determine the effects on gene expression. Subsequently, we transiently transfected ClC-3 cDNA or ClC-3-siRNA into MC3T3-E1 cells to determine the changed phenotype and gene expression. Lastly, we assessed the underlying mechanism responsible for ClC-3-induced osteodifferentiation. We found that ClC-3 mRNA was expressed in primary mouse osteoblasts and MC3T3-E1 cells and induced by using an osteoinductive procedure. We also found that overexpression of ClC-3 contributed to osteodifferentiation, such as increase in the expression of osteogenic markers [alkaline phosphatase (*Alp*), osteocalcin (*Oc*), bone sialoprotein (*Bsp*), osterix (*Osx*), and runt-related transcription factor 2 (*Runx2*)], morphological changes, and mineralized nodules in MC3T3-E1 cells. ClC-3 gene silencing suppressed gene expression of these osteogenic markers. Moreover, overexpressed ClC-3 protein co-localized with TGF-β1 in intracellular organelles, inhibited TGF-β1 protein expression and induced endosomal acidification. Nevertheless, knockdown of *Runx2* expression antagonized the effects of ClC-3 in osteodifferentiation and expression of osteogenic markers. The data from the current study suggest that the function of ClC-3 in osteodifferentiation may be through the Runx2 pathway. J. Cell. Biochem. 111: 49–58, 2010.

KEY WORDS: CHLORIDE CHANNELS; CLC-3; OSTEOGENESIS; OSTEODIFFERENTIATION; GENE REGULATION

The superfamily of ClC chloride channels are comprised of nine members in the mammals [Jentsch et al., 1999]. They are localized at plasma membranes or intracellular membrane junctions and function as Cl^- channels or H^+/Cl^- antiporters [Picollo and Pusch, 2005; Scheel et al., 2005]. Chloride channels display a variety of important physiological and biological roles, such as regulation of pH, volume homeostasis, organic solute transport, and cell migration, proliferation, and differentiation. The best evidence for their functional importance comes from human inherited diseases resulting from mutation in these channels. For example, ClC-1 is a candidate gene for myotonia [Kubisch et al., 1998]. Mutations of the ClC-5 gene cause Dent's disease with an impaired renal endocytosis

Abbreviations used: ClC-3, voltage gated chloride channel 3; *CLCN3* or *Clcn3*, ClC-3 chloride channel 3 gene; CLC-3, ClC-3 protein; ALP or *Alp*, alkaline phosphatase; BSP or *Bsp*, bone sialoprotein; OC or *Oc*, osteocalcin; *Runx2*, runt-related transcription factor 2; *Osx*, osterix; TGF-β1, transforming growth factor-beta 1.Huan Wang and Yong Mao contributed equally to this work.

Grant sponsor: Foundation of Key of Projects of Science and Technology of Xi'an City; Grant number: SF09027-4; Grant sponsor: Foundation of Key of Projects of Science and Technology of Shaanxi Province; Grant number: 2009K17-06.

*Correspondence to: Prof. Yin Ding, Department of Orthodontics, School of Stomatology, Fourth Military Medical University, Xi'an 710032, China. E-mail: dingyin@fmmu.edu.cn

**Correspondence to: Xiaohong Duan, Department of Oral Biology, School of Stomatology, Fourth Military Medical University, Xi'an 710032, China. E-mail: xhduan@fmmu.edu.cn

Received 29 January 2010; Accepted 13 April 2010 • DOI 10.1002/jcb.22658 • © 2009 Wiley-Liss, Inc.

Published online 23 April 2010 in Wiley Online Library (wileyonlinelibrary.com).

and kidney stone formation [Piwon et al., 2000] and mutations in the kidney-specific channel ClC-Kb lead to Batter's syndrome with severe salt wasting [Simon et al., 1997]. Mutations of ClC-7 or its β-subunit Ostm1 cause osteopetrosis associated with lysosomal storage disease [Lange et al., 2006].

Moreover, the disruption of ClC-3 expression causes a severe neurodegeneration with a dramatic loss of the hippocampus and the retina [Stobrawa et al., 2001]. *Clcn3*$^{-/-}$ mice are smaller than their littermates soon after birth, and exhibited skeletal abnormality, such as kyphoscoliosis, developmental retardation, and higher mortality [Yoshikawa et al., 2002]. ClC-3 can also reside in intracellular organelles of osteoclasts and contributes to bone resorption through organelle acidification [Okamoto et al., 2008]. These studies indicate that chloride channels, especially ClC-3 may play an important role in osteogenesis and phenotypes of bone metabolism [Gunther et al., 1998; Kornak et al., 2001; Yoshikawa et al., 2002].

ClC-3 was originally reported to be expressed in the brain, kidney, and many other tissues. The function of ClC-3 is thought to contribute to the acidification of synaptic vesicles, lysosomes, and endosomes in the tissues [Li et al., 2002; Hara-Chikuma et al., 2005]. However, recent findings suggest that ClC-3 plays a role in osteogenesis. Therefore, we investigated the novel role of ClC-3 in osteogenesis in this study. We detected ClC-3 expression in primary mouse osteoblasts and MC3T3-E1 cells. MC3T3-E1, a murine osteoprogenitor cell line, is usually used in researches on osteogenesis. Then, we performed an osteoinductive procedure and gene transfection of ClC-3 cDNA and siRNA, respectively to determine the changed phenotype and gene expressions in MC3T3-E1 cells. In addition, we also explored the underlying molecular mechanisms that are responsible for ClC-3-induced osteodifferentiation.

MATERIALS AND METHODS

CELL CULTURE AND OSTEOINDUCTION

MC3T3-E1 cells were obtained from Dr. Yan Zhang of the Department of Biochemistry and Molecular Biology at the Fourth Military Medical University, and cultivated in alpha-minimum essential medium (α-MEM, Gibco-Invitrogen, Grand Island, NY) containing 10% fetal bovine serum (FBS, Gibco), 100 U/ml penicillin G (Sigma, St. Louis, MO) and 100 μg/ml streptomycin (Sigma). Primary mouse osteoblasts were prepared by sequential digestion of murine calvarias as described previously [Bakker and Klein-Nulend, 2003] and cultivated in Dulbecco Modified Eagle's Minimal Essential Medium (DMEM) supplemented with 10% FBS, 100 U/ml of penicillin, and 100 μg/ml of streptomycin in a humidified incubator at 37°C with 95% air and 5% CO_2. The cells were subcultured every 72 h using 0.25% trypsin plus 0.02% EDTA (Gibco) in phosphate-buffered saline (PBS, Gibco). For the osteoinductive procedure, cells were cultured in osteogenic medium, that is, α-MEM with 10% FBS, 50 μg/ml ascorbic acid (Gibco), 10 mM β-glycerol-phosphate (Gibco) and 10 nM dexamethasone (Sigma).

CLC-3 PLASMID AND GENE TRANSFECTION

pCMV-clcn3-HA carrying a full-length mouse *Clcn3* cDNA was a gift from Dr. Sandra. E. Guggino of Johns Hopkins University. For gene transfection, MC3T3-E1 cells were plated at 1×10^4 cells/ml cultured in α-MEM supplemented with 10% FBS in six-well plates overnight and were transfected with ClC-3 plasmid or pCMV-HA plasmid as a control [Field et al., 1988] with Lipofectamine 2000 (Invitrogen, Carlsbad, CA). The culture medium was renewed after 8 h incubation. After 48 h, the cells were collected for the following described experiments.

CLC-3 SIRNA AND GENE SILENCING

The small interfering RNA (siRNA) duplexes that target the mouse ClC-3 were designed and synthesized by GenePharma (Shanghai, China) according to GenBank™ (AF029347) (sense, 5′-CGA GAG AAG UGU AAG GAC ATT-3′ and antisense, 5′-UGU CCU UAC ACU UCU CUC GTT-3′). The nonsense siRNA sequence (sense, 5′-UUC UCC GAA CGU GUC ACG UTT-3′ and antisense, 5′-ACG UGA CAC GUU CGG AGA ATT-3′) was used as a control. For gene transfection, MC3T3-E1 cells were plated at 1×10^4 cells/ml in α-MEM supplemented with 10% FBS in six-well plates overnight and were transfected with the siRNA duplexes using Lipofectamine 2000 and the final siRNA concentration was 100 nM. After 5 h transfection, the growth medium was refreshed with the regular growth medium and total RNA from the cells was isolated 72 h later for gene expression.

RUNX2 SIRNA AND GENE SILENCING

Runx2 siRNA was synthesized and prepared by GenePharma (Shanghai, China) according to GenBank™ sequences NM 009820 (*Runx2* sense, 5′-GAA GCU UGA CUC UAA ATT-3′; antisense, 5′-UUU AGA GUC AUC AAG CUU CTG-3′). In addition, a siRNA from GenePharma with sense 5′-UCC UCC GAA CGU GUC ACG UTT-3′ and antisense 5′-ACG UGA CAC GUU CGG AGA ATT-3′ served as a "scrambled" control. The siRNA duplexes were transfected into the cells using Lipofectamine 2000 and the final siRNA concentration was 100 nM. Total RNA of cells was extracted after 72 h incubation with siRNA.

WESTERN BLOT ANALYSIS

The cells were lysed in a buffer containing 0.05 M Tris (pH 7.4), 0.15 M NaCl, 1% Nonidet P-40, 1 mM EDTA, 1 μg/ml leupeptin, 1 μg/ml aprotinin, and 1 mM phenylmethyl sulfonyl fluoride. The protein concentration was determined using BCA reagent (Pierce, Rockford, IL). After this, 50 μg of the total protein lysate were separated via sodium dodecyl sulfate–polyacrylamide gel electrophoresis and transferred to a PVDF membrane (Millipore, Billerica, MA). The PVDF membranes then were subjected to Western blot analysis. Briefly, the membrane was first blocked in a Tris-buffered solution (TBS) containing 5% non-fat milk for 30 min, and in anti-HA-tag monoclonal antibody (Cell Signaling technology, Boston, MA,), mouse anti-TGF-β1 antibody (R&D Systems, Minneapolis, MN) or anti-β-actin rabbit polyclonal antibody (Boster, Wuhan, China) overnight. After washing, the membranes were incubated at room temperature in a fluorophore-labeled goat-anti-mouse secondary antibody (IRDye680, LI-COR, Lincoln, NE). Bands were detected and quantified on the Odyssey image system (LI-COR).

RNA EXTRACTION, RT-PCR, AND REAL-TIME PCR

Total cellular RNA was extracted with TRIzol® Reagent (Invitrogen) according to the manufacturer's protocol. A reverse transcriptase cDNA synthesis kit (TaKaRa, Dalian, China) was used to synthesize

TABLE I. Primers Sequences and Expected Size of PCR Products

Genes	Forward primer	Reverse primer	Size (bp)
Clcn3	5′-CCAAGACCCCGCTTCAATAA-3′	5′-CGAGTCCCGCAGATTAAAGA-3′	112
Alp	5′-CCAACTCTTTTGTGCCAGAGA-3′	5′-GGCTACATTGGTGTTGAGCTTTT-3′	110
Bsp	5′-CAGGGAGGCAGTGACTCTTC-3	5′-AGTGTGGAAAGTGTGGCGTT-3′	158
Oc	5′-CTGACCTCACAGATCCCAAGC-3′	5′-TGGTCTGATAGCTCGTCACAAG-3′	187
Runx2	5′-CGCCCCTCCCTGAACTCT-3′	5′-TGCCTGCCTGGGATCTGTA-3′	72
Osx	5′-ATGGCGTCCTCTCTGCTTG-3′	5′-TGAAAGGTCAGCGTATGGCTT-3′	156
Gapdh	5′-CATGTTCCAGTATGACTCCACTC-3′	5′-GGCCTCACCCCATTTGATGT-3′	136

cDNA and amplified in Veriti™ 96-well Thermal Cycler (Applied Biosystems, Foster, CA) with specific primers (Table I). The PCR products were then electrophoresed in 1.5% agarose gel and visualized by ethidium bromide under the UV light. Expression levels of target genes were further determined quantitatively by an ABI 7500 real-time PCR system (Applied Biosystems) using SYBR® Premix Ex Tag™ (TaKaRa). Total cDNA (10–30 ng) was added per 20 μl reaction. Thermocycling conditions were set to the following: 95°C for 30 s; 45 cycles at 95°C for 5 s, 60°C for 34 s. The primers used are listed in Table I. Quantification of gene expression was performed using the comparative threshold cycle ($\Delta\Delta C_T$) method [Livak and Schmittgen, 2001] and the relative expression levels were quantified by comparing the ratios to the reference gene, *Gapdh* cycle threshold (C_T).

ALIZARIN RED S STAINING AND QUANTIFICATION

Alizarin Red S staining was used to determine mineralization levels in the cells. In order to observe a long-term gene transfection effect, transient transfection of pCMV-clcn3-HA was repeated six times every 3 days for 21 days. Mock-transfected cells were used as a control. After 21 days, the cells were fixed and stained with 2% Alizarin Red S (pH 4.2, Sigma). The images were taken using an Olympus interlined CCD camera (Olympus, Tokyo, Japan), and analyzed with a Leica Q-Win image analysis system (Leica Microsystems, Germany).

IMMUMOFLUORESCENCE ANALYSIS

MC3T3-E1 cells were grown on glass coverslips and transfected with ClC-3 expression plasmid and 2 days later, they were fixed with 4% paraformaldehyde for 20 min at 4°C and permeabilized with 0.03% Triton X-100 in PBS for 30 min. The coverslips were incubated with rabbit polyclonal anti-mouse HA-tag antibody (at a dilution of 1:500, Thermo Scientific, Fremont, CA) or mouse anti-TGF-β1 antibody (at a dilution of 1:300, R&D Systems) overnight at 4°C after blockade of nonspecific binding with 10% rabbit serum for 30 min at room temperature. In the next day, the coverslips were washed with PBS for three times and then incubated with fluorescein (FITC) affinity-pure donkey anti-mouse IgG (at a dilution of 1:300, Jackson ImmunoResearch, West Grove, PA) or Cy3 labeled goat anti-rabbit IgG polyclone antibody (at a dilution of 1:200, Jackson ImmunoResearch) for 60 min at 37°C. Nuclear counterstaining was performed with Hoechst 33342 (at a dilution of 1:1,000, Sigma). After rinsed with PBS, the coverslips were reviewed under a FluoView FV1000 laser confocal microscope (Olympus). In order to analyze the intensities of fluorescence of staining for TGF-β1 protein, an Olympus IX71 microscope was also used to capture pictures. Fifty cells in each group were counted and intensities of positive TGF-β1 staining were measured and analyzed with Image J 1.42 software (Wayne Rasband, NIH, USA).

ANALYSIS OF CELLULAR PH VALUE

To determine intracellular pH value, the cells were exposed to LysoSensor™ DND-167 (Invitrogen). The LysoSensor™ reagents exhibit a pH-dependent increase in fluorescence intensity upon acidification. Briefly, MC3T3-E1 cells were grown and transfected with ClC-3 cDNA or pCMV-HA plasmid. After that, the cells were briefly washed with PBS (pH 7.4) twice and then incubated with DND-167 (3 μM) at 37°C with 95% air and 5% CO_2 for 60 min and reviewed under a FluoView FV1000 confocal microscope (Olympus) with UV excitation. Images were also captured with an Olympus IX71 microscope. The intensity of intracellular fluorescence was analyzed with NIH Image J 1.42 software and more than 50 cells were counted in each group.

STATISTICAL ANALYSIS

Data were presented as mean ± SEM. Comparative studies of means were performed using one-way analysis of variance followed by a post-hoc test (projected least significant difference Fisher). Student's *t*-tests were used when only two groups were compared. Values of *P* less than 0.05 were considered to be statistically significant.

RESULTS

INCREASED EXPRESSION OF CLC-3 MRNA AFTER OSTEOINDUCTIVE TREATMENT

We first determined the levels of ClC-3 mRNA expression in mouse osteoprogenitor cells and primary mouse osteoblasts. RT-PCR analysis shows that an expected cDNA size (112 bp) corresponding to mouse ClC-3 is clearly amplified in RNA isolated from mouse osteoprogenitor MC3T3-E1 cells and primary mouse osteoblasts (Fig. 1A). To assess levels of ClC-3 and other osteogenic-related gene expression after induction of osteodifferentiation in MC3T3-E1 cells, we performed the osteoinductive procedure and the data indicated that after 48 h osteoinduction, *Clcn3* expression was significantly induced, together with other osteogenic-related genes using real-time PCR analysis (Fig. 1B). Level of *Clcn3* mRNA, a mouse homolog of human ClC-3, increased more than threefold in osteogenic medium compared to the control culture. In addition, *Bsp*, an osteodifferentiation marker is also induced by 10-fold after the osteoinductive procedure, while other osteogenic markers (such as *Alp*, *Oc* and *Runx2*) were induced 3-, 2.6-, and 2.7-fold, respectively.

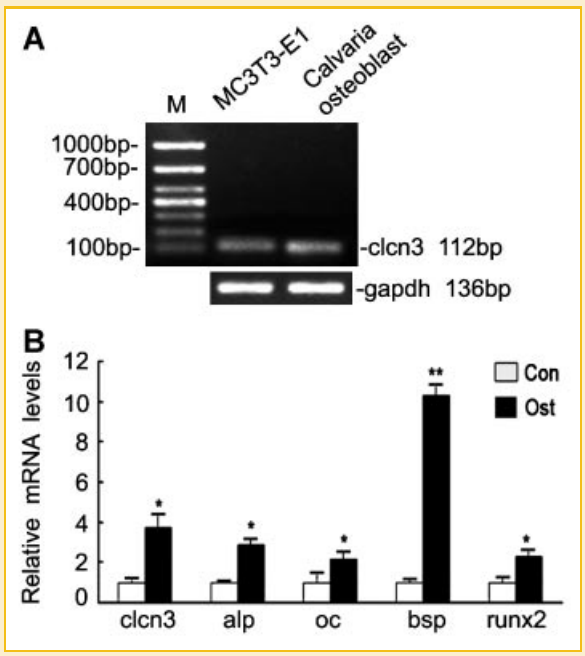

Fig. 1. Effects of osteoinduction on the regulation of *Clcn3* and expression of the osteogenic markers. A: RT-PCR results. MC3T3-E1 cells and primary mouse osteoblasts were cultivated and RNA was extracted from the cells and subjected to RT-PCR analysis of ClC-3 expression. The size of PCR products of *Clcn3* and *Gapdh* were 112 bp and 136 bp, respectively. M: DNA Marker DL1,000 (TaKaRa, Dalian, China). B: Real-time PCR results. MC3T3-E1 cells were grown in control nonosteoinductive medium (Con) or osteoinductive medium (Ost) for 48 h and RNA from the cells was extracted and subjected to real-time PCR analysis of gene expression. $^{*}P < 0.05$, $^{**}P < 0.01$, $n = 3$.

EFFECTS OF CLC-3 IN OSTEODIFFERENTIATION OF MC3T3-E1 CELLS

To investigate the biological functions of ClC-3 in MC3T3-E1 cells and its role in regulating the expression of osteogenic-related genes, we transiently transfected a full length *Clcn3* cDNA into MC3T3-E1 cells. The data showed that ClC-3 gene expression was significantly increased in the transfected cells, as detected by real-time PCR analysis (Fig. 2A). Western blot data showed the positive HA-tag expression in pCMV-clcn3-HA-transfected cells versus mock-transfected cells (Fig. 2C). The following data further indicated that overexpression of ClC-3 upregulated levels of *Bsp* and *Oc* mRNA by 8.3- and 7.8-fold, respectively, while *Alp* expression was induced by 3.3-fold and *Runx2* level by 1.8-fold compared to the control group (Fig. 2D).

To confirm the contribution of ClC-3 in osteogenic differentiation, we further examined the effects of ClC-3 siRNA on the cells and found the efficiency and specificity of ClC-3 siRNA transfection and the changed gene expression of osteogenic markers by using real-time PCR analysis. ClC-3 siRNA was able to knockdown 81% of ClC-3 gene expression (Fig. 2B). The expression of these osteogenic markers was significantly reduced to 25–63% of normal levels in the ClC-3 gene silencing cells compared to the nonsense transfection control cells using real-time PCR analysis (Fig. 2E).

Furthermore, we also determined calcium deposition of extracellular matrix and morphology changes in MC3T3-E1 cells after ClC-3 gene transfection. After 21 days of six-time transfections of ClC-3 cDNA, calcium nodules was significantly increased in MC3T3-E1 cells (Fig. 3C), compared to the control group (Fig. 3B). Alizarin Red S positive staining area per microscopic field was 38.4% in the presence of ClC-3 plasmid (Fig. 3C) and 7.6% in controls (Fig. 3B),

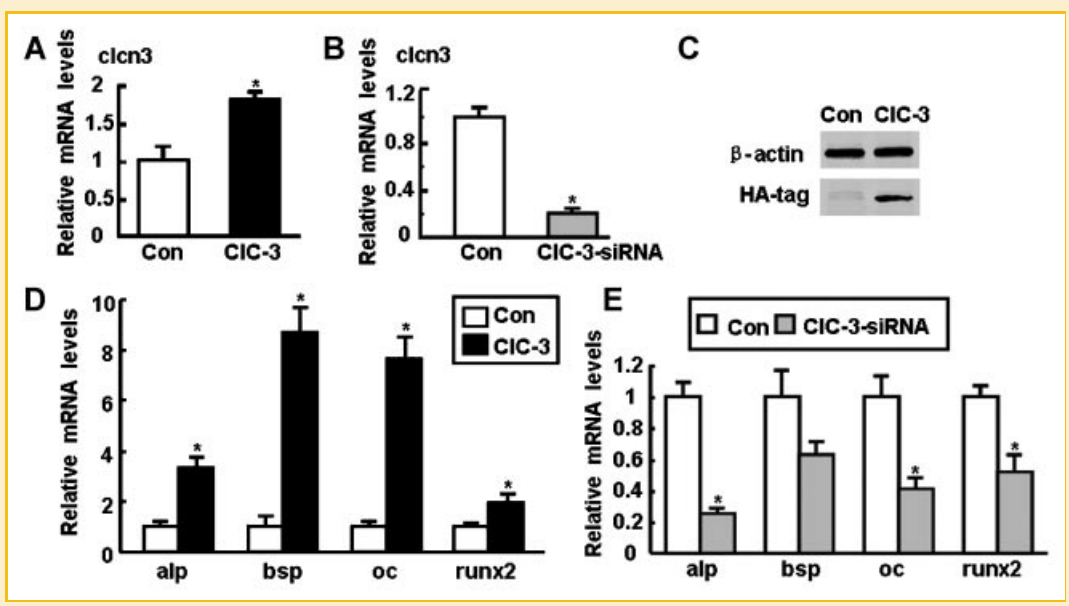

Fig. 2. Effects of ClC-3 on expression of the osteogenic markers. A: Real-time PCR result. MC3T3-E1 cells were transiently transfected with or without ClC-3 cDNA and total cellular RNA was then extracted and subjected to real-time PCR analysis of Clcn3 expression. B: Efficiency of ClC-3 gene silencing. Clcn3 expression was significantly suppressed by ClC-3 siRNA using real-time PCR analysis. C: Western blot results. MC3T3-E1 cells were grown and transiently transfected with a pCMV-clcn3-HA plasmid (ClC-3) and total cellular protein was isolated and subjected to Western blot analysis of CLC-3 protein expression with HA-tag antibody. D,E: Real-time PCR results. Gene expression was normalized by *Gapdh* expression. Gene expression level in cells transfected with pCMV-HA plasmid or nonsense siRNA was considered to be 1. Gene expression of the osteogenic markers was increased in ClC-3 overexpressed cells but was reduced after ClC-3 gene silence. $^{*}P < 0.05$, $n = 3$. [Color figure can be viewed in the online issue, which is available at wileyonlinelibrary.com.]

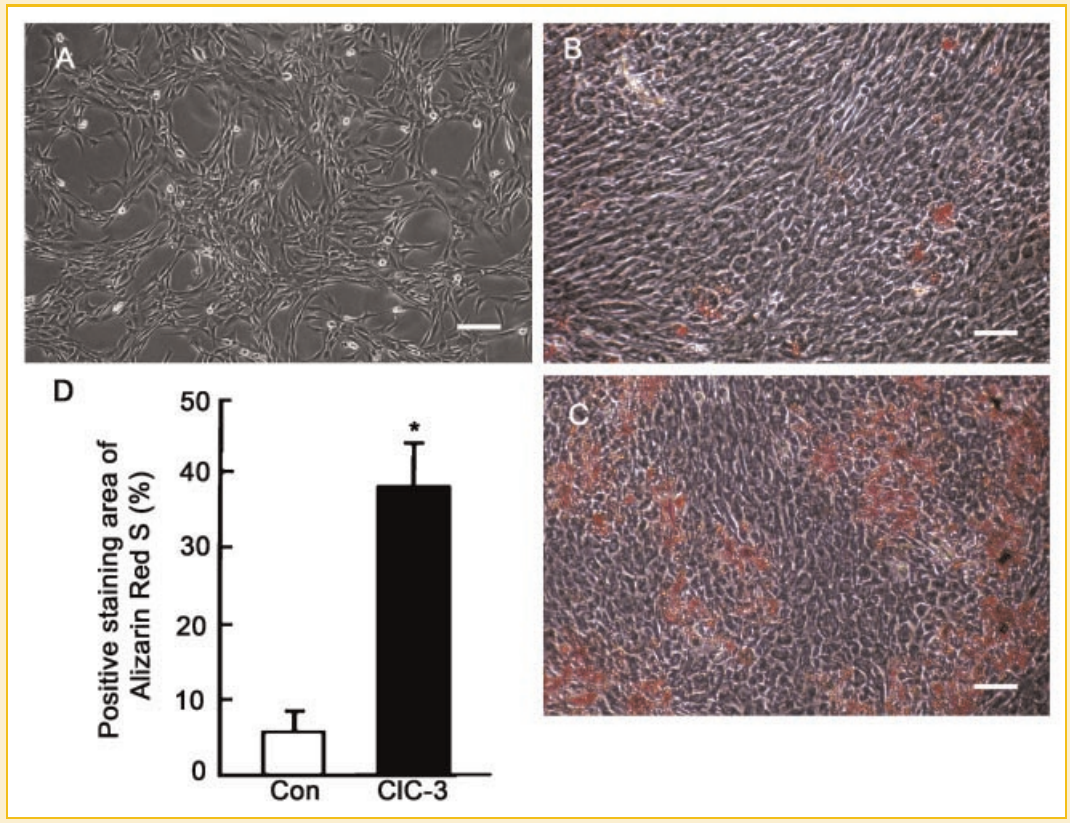

Fig. 3. Effects of the overexpression of ClC-3 on the mineralization of MC3T3-E1 cells. A: Morphology of MC3T3-E1 cells in α-MEM before ClC-3 overexpression. The cells are slender and spindle-shaped. B,C: Alizarin Red S staining of MC3T3-E1 cells. MC3T3-E1 cells were grown and repeated transfected with pCMV-HA plasmid (B) or ClC-3 cDNA (C) for 21 days. Bars = 50 μm. ClC-3 overexpressing cells showed the cuboidal osteoblast state and more calcified nodules in red. D: Quantification of positive Alizarin Red S staining data. The Y-axis is the positive staining area per microscopic field. Results are expressed as mean ± SEM. $^{*}P < 0.05$, n = 3. [Color figure can be viewed in the online issue, which is available at wileyonlinelibrary.com.]

respectively. Morphologically, MC3T3-E1 cells overexpressing ClC-3 switched, from pre-osteoblast fibroblastoid state (Fig. 3A,B) to cuboidal early osteoblasts after 21-day cultivation (Fig. 3C).

CO-LOCALIZATION OF CLC-3 PROTEIN WITH TGF-*B*1

It has been reported that ClC-3 channel predominately localized in endosomal system in many types of the cells [Stobrawa et al., 2001; Li et al., 2002; Hara-Chikuma et al., 2005; Okamoto et al., 2008]. After transfected with pCMV-clcn3-HA, we detected the HA-tag expression to determine the subcellular localization of CLC-3 protein and the co-localization of CLC-3 with TGF-β1 using a confocal laser scanning microscope. Figure 4 shows the double immunostaining of MC3T3-E1 cells with antibodies against HA-tag and TGF-β1. As known in the merge imagine (Fig. 4D,H), the HA-tag signal was prominently seen in the cell periphery and co-localized with TGF-β1.

CLC-3 INHIBITS OF TGF-*B*1 PROTEIN EXPRESSION

To understand the mechanism of the regulation of TGF-β1 by ClC-3, we analyzed the expression of TGF-β1 protein by Western blot. The expression of TGF-β1 protein was decreased significantly in cells transfected with pCMV-clcn3-HA compared to the mock-transfected cells and pCMV-HA plasmid transfection group (Fig. 5). After analysis of intensities of fluorescence of TGF-β1 signal among these three groups in immunofluorescence staining experiments, we found that expression of TGF-β1 in cells overexpressed with ClC-3 was also significantly decreased compared to the other two groups, suggesting that the expression of TGF-β1 has no difference between mock-transfection group and empty plasmid transfection group (Fig. 4M).

CLC-3 INDUCTION OF INTRACELLULAR ACIDIC ENVIRONMENT IN MC3T3-E1 CELLS

In addition, we assessed intracellular pH value using LysoSensor™ Blue DND-167 staining. We found that the intracellular perinuclear vesicles exhibited stronger blue fluorescence staining after over-expression of ClC-3 (Fig. 6B), suggesting a decreased pH value in the cells. Quantitatively, intensity of fluorescence in the cells transfected with ClC-3 was significantly increased by 8.7-fold compared to the control group (Fig. 6E). However, there are no significant differences in fluorescence intensity between the osteoinductive cells (Fig. 6D) and the non-osteoinductive cells (Fig. 6C), indicating that the osteoinductive procedure did not have an effect on the intracellular pH value, at least when examined within 48 h.

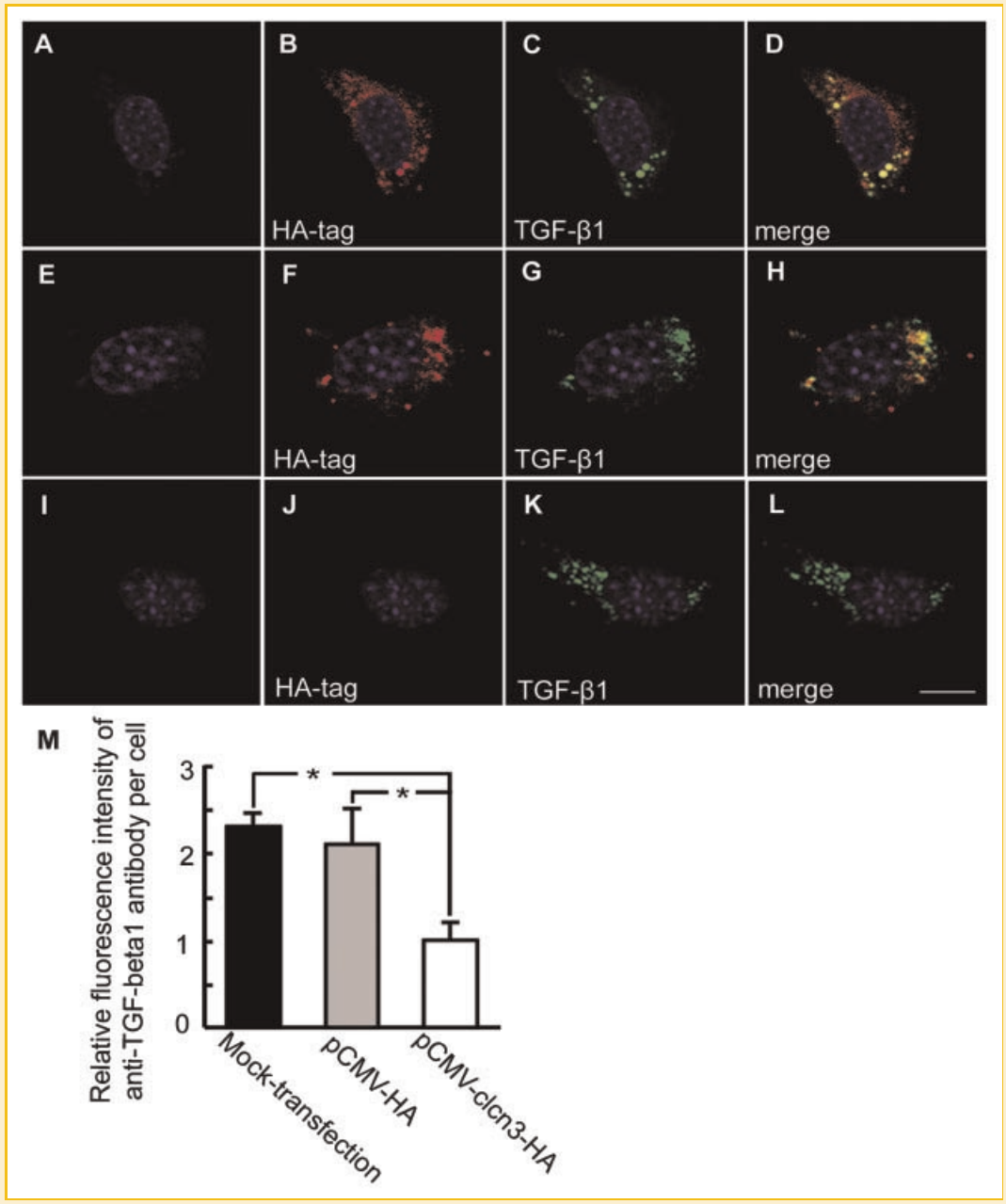

Fig. 4. Co-localization of CLC-3 protein with TGF-β1 in MC3T3-E1 cells. MC3T3-E1 cells were mock-transfected, transfected with pCMV-clcn3-HA plasmid or pCMV-HA plasmid and then doubleimmunostained with anti-HA-tag and anti-TGF-β1 antibodies, followed by Cy3 labeled goat anti-rabbit IgG polyclone antibody (shown as red) and FITC labeled donkey anti-mouse IgG (shown as green). A–D: Cells transfected with pCMV-clcn3-HA plasmid and viewed under an Olympus confocal laser scanning microscope FV1000. E–H: Cells transfected with pCMV-HA plasmid. I–L: Cells in mock-transfection. Nuclei (blue) were stained with Hoechst 33342. Co-localization of HA-tag (red) and TGF-β1 (green) are indicated as yellow in the intracellular organelles (D,H). Bars = 20 μm. M: Intensities of fluorescence of TGF-β1 signal among three groups. The cells were also reviewed under an Olympus IX71 microscope to capture pictures and the fluorescence intensities of 50 cells of each group were analyzed. The data were summarized as the average fluorescence intensity of positive TGF-β1 staining per cell. $^{*}P < 0.05$. [Color figure can be viewed in the online issue, which is available at wileyonlinelibrary.com.]

RUNX2 SILENCING INTERRUPTS CLC-3 REGULATED OSTEODIFFERENTIATION

Our data presented so far clearly indicate that ClC-3 can promote the osteogenic differentiation and mineralization of MC3T3-E1 cells. Next, we determined the underlying molecular pathway responsible for ClC-3-induced osteodifferentiation. We synthesized and transfected the *Runx2* siRNA into MC3T3-E1 cells and the data showed approximately 70% reduction of *Runx2* mRNA. It was not surprising that the levels of *Alp*, *Bsp*, *Oc*, and *Osx* mRNA were all reduced to 24–44% of normal levels in the *Runx2* silencing group compared to the scrambled transfection control group by real-time PCR analysis (Fig. 7). In addition, we also compared the expression of these genes after overexpression of ClC-3, and levels of *Alp*, *Bsp*, *Oc*, *Osx*, and *Runx2* mRNA were increased by 3.2-, 4.9-, 4.4-, 2.1-, and 1.8-fold,

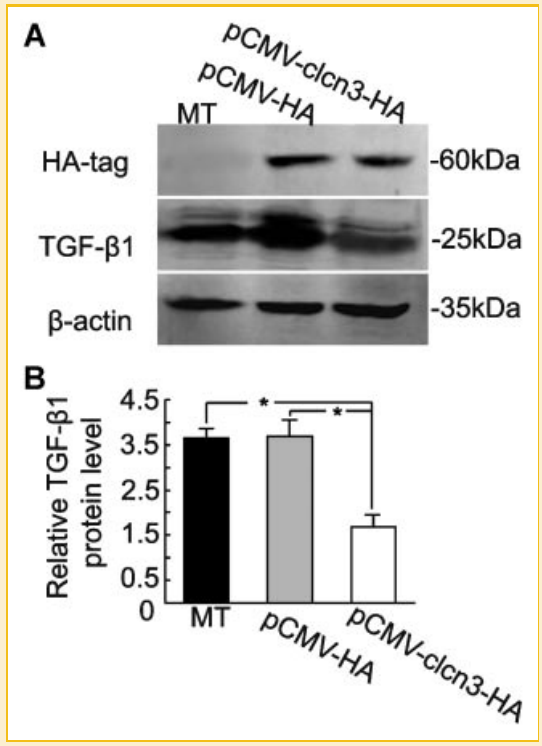

Fig. 5. ClC-3 inhibits TGF-β1 protein expression. A: Western blot results. MC3T3-E1 cells were mock-transfected (MT) and transiently transfected with pCMV-clcn3-HA plasmid (pCMV-clcn3-HA) or pCMV-HA plasmid (pCMV-HA), and total cellular protein was isolated and subjected to Western blot analysis. B: TGF-β1 protein level was decreased in cells transfected with pCMV-clcn3-HA plasmid compared to the cells transfected with pCMV-HA plasmid or mock-transfected. $^{*}P < 0.05$, n = 3. [Color figure can be viewed in the online issue, which is available at wileyonlinelibrary.com.]

respectively, compared to the control group. Co-transfection of ClC-3 cDNA and *Runx2* siRNA resulted in a reduction (40–75%) of the expression of the osteogenic markers, indicating that *Runx2* siRNA antagonized the effects of ClC-3 in the gene expression of these markers (Fig. 7).

DISCUSSION

In this study, we have demonstrated that ClC-3 is expressed in MC3T3-E1 cells and in primary mouse osteoblasts. We further observed the effects of ClC-3 overexpression and ClC-3 gene silencing on osteogenic differentiation of MC3T3-E1 cells. Molecularly, Runx2 can interrupt the role of ClC-3 during osteogenic differentiation. To the best of our knowledge, this is the first report that associates ClC-3 channel with osteogenic differentiation.

ClC-3 contributes to endosomal acidification and also plays important roles in physiological functions in the cells. Silence of ClC-3 effectively inhibits cell proliferation in rat basilar arterial smooth muscle cells [Tang et al., 2008]. ClC-3 is considered to participate in the fibroblast-to-myofibroblast transition [Yin et al., 2008]. ClC-3 inhibits human bronchial epithelial cell apoptosis [Cheng et al., 2007]. Both ClC-3 and ClC-7 have been reported to be highly expressed in osteoclasts [Kornak et al., 2001; Okamoto et al., 2008], suggesting that they may have a role in osteogenesis, where the latter is involved in the balance of bone formation and resorption. Moreover, Cl^- current has previously been described to stimulate the proliferation of MC3T3-E1 cells [Maki et al., 2007], but the correlative role of Cl^- in cell differentiation remains to be determined. Since ClC-3 regulates intracellular Cl^- levels, the ClC-3 gene may also play a role in cell growth and differentiation. Our current study confirmed this hypothesis. We found that the expression of *Clcn3* was significantly induced together with the increase in expression of other osteogenic-related genes after the osteoinductive procedure in MC3T3-E1 cells. We utilized osteogenic-related genes to assess osteodifferentiation after the osteoinductive procedure, in accordance with previous reports showing an increased expression of these genes during osteodifferentiation [Quarles et al., 1992; Alford and Hankenson, 2006]. In the current study, transfection of ClC-3 cDNA into MC3T3-E1 cells has a similar effect of the osteoinductive procedure, which demonstrated that ClC-3 plays a role in regulation of osteogenic-related markers during osteodifferentiation. Moreover, ClC-3 gene silencing significantly suppressed gene expression of these osteogenic markers, which further implys the role of ClC-3 in regulation of osteodifferentiation. In addition, ClC-1 was recently reported to regulate osteoblastic differentiation from mesenchymal progenitor cells [Yang et al., 2009]. Furthermore, we followed the protocol for cultivated MC3T3-E1 cells and transiently transfected ClC-3 cDNA for 21 days with six-time transfections because it has been reported that MC3T3-E1 cells take 5–16 days to differentiate into mature osteoblasts [Quarles et al., 1992]. We found that overexpression of ClC-3 increased the number of calcium nodules and altered cell morphology during the 21-day culture, further indicating that ClC-3 promoted osteodifferentiation and mineralization of MC3T3-E1 cells.

In addition, ClC-3, ClC-4, and ClC-5 are predominately present on intracellular membranes [Scheel et al., 2005]. Their high degree of sequence similarity and common functions strongly suggest that ClC-3 may function as an H^+/Cl^- exchanger, like ClC-4 and ClC-5 [Picollo and Pusch, 2005; Jentsch, 2007]. Moreover, ClC-3 has also been reported to provide shunt conductance that permits intraluminal acidification by the V-ATPase [Jentsch, 2007]. Inward chloride conduction has been shown to enhance acidification in endosomes and acidification is mediated through V-type ATPase pumping protons into the organelle lumen [Grabe and Oster, 2001]. During ascorbic acid-induced differentiation of osteogenic cells, total lysosome organelles obviously increase. The impairment of lysosome dispersion markedly reduced the osteodifferentiation [Nabavi et al., 2008]. Typically, the enhanced fluorescence indicated that overexpression of ClC-3 might facilitate the acidification of endosomes, which supported previous studies in CHO-K1, Huh-7, hepatocytes, osteoclasts and other types of cells [Li et al., 2002; Hara-Chikuma et al., 2005; Okamoto et al., 2008]. The impaired endosomal acidification was also demonstrated in the ClC-3-deficient mice [Okamoto et al., 2008]. The data from the current study suggest that overexpression of ClC-3 may accumulate Cl^- to control the pH value of intracellular vesicles and provide a suitable intracellular environment for osteoinduction.

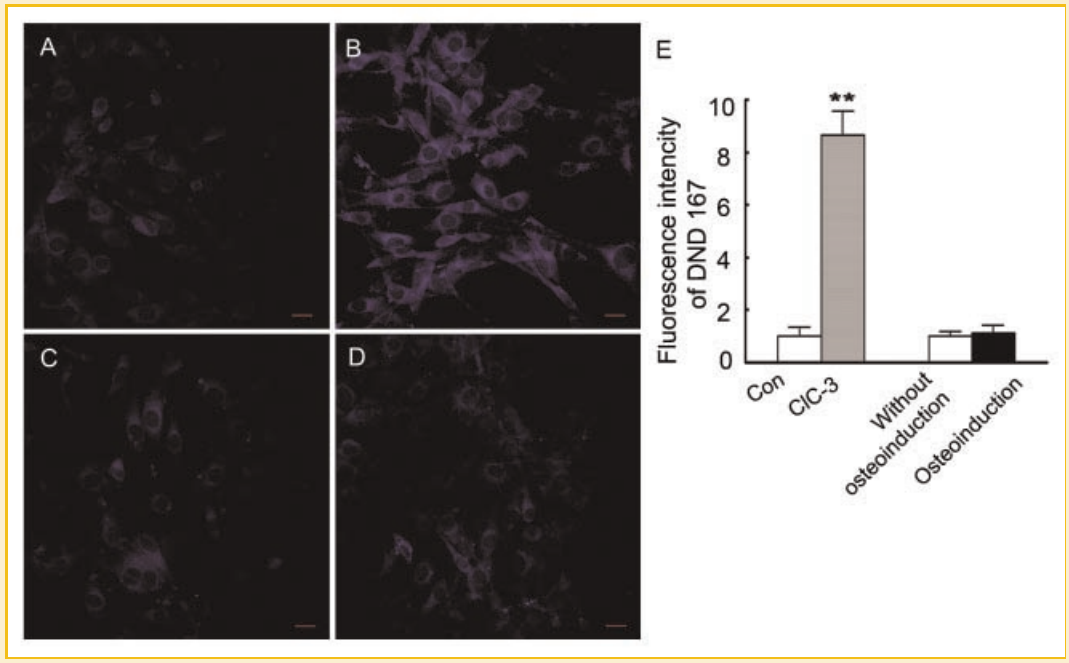

Fig. 6. Effects of the overexpression of ClC-3 on the regulation of the intracellular pH value. A–D: MC3T3-E1 cells were grown and transiently transfected with pCMV-HA plasmid (A) or pCMV-clcn3- HA plasmid (B) and stained with fluorescence dye DND-167. In addition, MC3T3-E1 cells were grown in control non-osteoinductive medium (C) or in osteoinductive medium (D). Bars = 20 μm. E: The data were summarized as the average fluorescence intensity of DND-167 staining per cell. $^{**}P < 0.01$. [Color figure can be viewed in the online issue, which is available at wileyonlinelibrary.com.]

TGF-β1 is an important regulator in physiological functions of cells and many researches have referred to the relationship of TGF-β1 and ClCs. Overexpression of ClC-3 significantly inhibited TGF-β1-induced apoptosis in human bronchial epithelial cells [Cheng et al., 2007]. Our recent study found that ClC-5 regulated tooth development through TGF-β1 signal pathway [Duan et al., 2009]. In present study, we showed the co-localization of ClC-3 and TGF-β1 protein in perinuclear and intracellular organelles, such as endosomes and lysosomes. Our data also showed that over-expression of ClC-3 significantly decreased the expression of TGF-β1, which might be correlated with the changed intracellular microenvironment for ClC-3 overexpressing. Strong acid or base was reported to be capable of activating the maximum of TGF-β present in fibroblastic cell-conditioned medium [Lyons et al., 1988].

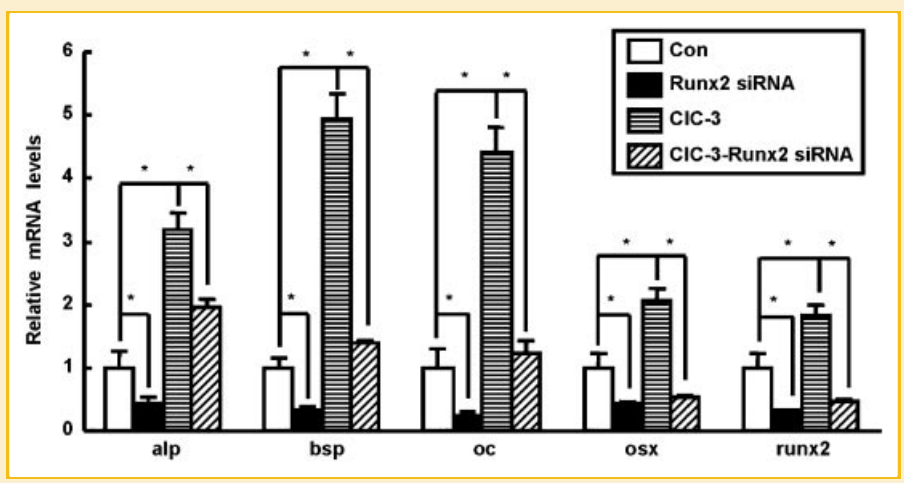

Fig. 7. EEffects of the Runx2 siRNA on the regulation of gene expression. MC3T3-E1 cells were grown and transiently transfected with plasmid-only (con), Runx2 siRNA, (Runx2 siRNA) ClC-3 cDNA (ClC-3), or Runx2 siRNA plus ClC-3 cDNA (ClC-3 - Runx2 siRNA), then RNA was extracted from the cells and subjected to real-time RT-PCR analysis of gene expression. $^{*}P < 0.05$, n = 3.

Overexpression of ClC-3 promoted the endosomal acidification. A change in pH might have a physiological effect on latent TGF-β and to lead to increased TGF-β degradation.

In our current data, we showed that expression of *Runx2* was significantly upregulated after the osteoinductive procedure and ClC-3 overexpression in MC3T3-E1 cells. As a master transcription regulator of the osteoblast, Runx2 has the ability to induce the expression of multiple osteogenic marker genes including type I collagen, OC, BSP, and osteopotin [Ducy et al., 1997; Otto et al., 1997; Lamour et al., 2007]. In order to test whether ClC-3 regulated the osteogenic-related gene expression through the Runx2 pathway, we used *Runx2* siRNA to knockdown the *Runx2* mRNA level. After *Runx2* expression was suppressed, the ClC-3-regulated osteodifferentiation was blocked or inhibited. Runx2 is a demonstrated part of the transcriptional stimulatory cascade of Osx, another important transcription regulator in osteodifferentiation [Tu et al., 2006]. In the present study, the level of *Osx* mRNA was decreased when *Runx2* knockdown, which suggests that *Osx* is a downstream gene of *Runx2* [Nakashima et al., 2002; Komori, 2006]. Moreover, TGF-β and Runx2 have important interactions in osteogenesis, for instance TGF-β1 inhibits osteoblast differentiation through Smad3-mediated repression of Runx2 function [Alliston et al., 2001; Komori, 2006; Franceschi et al., 2009]. It needs further investigation to elucidate the molecular mechanism of ClC-3 in osteogenesis.

In conclusion, the endosomal chloride channel ClC-3 has a relationship with the expression of osteogenic markers during osteogenesis, promotes the mineralization of MC3T3-E1 cells, takes part in endosomal acidification and downregulates TGF-β1 protein level. Furthermore, Runx2 siRNA blocked the function of ClC-3 in the upregulation of gene expression in osteodifferentiation. The results from our current study suggest that the role of ClC-3 in osteodifferentiation may be through the Runx2 gene pathway, which in turn mediates bone formation and remodeling. Further investigation will elucidate the underlying mechanisms and potential use of ClC-3 as a therapeutic target for treatment of osteogenesis-related diseases.

ACKNOWLEDGMENTS

We would like to thank Dr. Sandra E. Guggino of Johns Hopkins University for providing the ClC-3 expression plasmid, Dr. Yan Zhang of the Department of Biochemistry and Molecular Biology at the Fourth Military Medical University for providing MC3T3-E1 cells, and Equipment Center of PLA Institute of Stomatological Research for their kindly technique support. This study was supported in part by the Foundation of Key of Projects of Science and Technology of Xi'an City [#SF09027(4)] and the Foundation of Key of Projects of Science and Technology of Shaanxi Province (#2009K17-06).

REFERENCES

Alford AI, Hankenson KD. 2006. Matricellular proteins: Extracellular modulators of bone development, remodeling, and regeneration. Bone 38:749–757.

Alliston T, Choy L, Ducy P, Karsenty G, Derynck R. 2001. TGF-beta-induced repression of CBFA1 by Smad3 decreases cbfa1 and osteocalcin expression and inhibits osteoblast differentiation. EMBO J 20:2254–2272.

Bakker A, Klein-Nulend J. 2003. Osteoblast isolation from murine calvariae and long bones. Methods Mol Med 80:19–28.

Cheng G, Shao Z, Chaudhari B, Agrawal DK. 2007. Involvement of chloride channels in TGF-beta1-induced apoptosis of human bronchial epithelial cells. Am J Physiol Lung Cell Mol Physiol 293:L1339–L1347.

Duan X, Mao Y, Yang T, Wen X, Wang H, Hou J, Xue Y, Zhang R. 2009. ClC-5 regulates dentin development through TGF-beta1 pathway. Arch Oral Biol 54:1118–1124.

Ducy P, Zhang R, Geoffroy V, Ridall AL, Karsenty G. 1997. Osf2/Cbfa1: A transcriptional activator of osteoblast differentiation. Cell 89:747–754.

Field J, Nikawa J, Broek D, MacDonald B, Rodgers L, Wilson IA, Lerner RA, Wigler M. 1988. Purification of a RAS-responsive adenylyl cyclase complex from Saccharomyces cerevisiae by use of an epitope addition method. Mol Cell Biol 8:2159–2165.

Franceschi RT, Ge C, Xiao G, Roca H, Jiang D. 2009. Transcriptional regulation of osteoblasts. Cells Tissues Organs 189:144–152.

Grabe M, Oster G. 2001. Regulation of organelle acidity. J Gen Physiol 117:329–344.

Gunther W, Luchow A, Cluzeaud F, Vandewalle A, Jentsch TJ. 1998. ClC-5, the chloride channel mutated in Dent's disease, colocalizes with the proton pump in endocytotically active kidney cells. Proc Natl Acad Sci USA 95:8075–8080.

Hara-Chikuma M, Yang B, Sonawane ND, Sasaki S, Uchida S, Verkman AS. 2005. ClC-3 chloride channels facilitate endosomal acidification and chloride accumulation. J Biol Chem 280:1241–1247.

Jentsch TJ. 2007. Chloride and the endosomal-lysosomal pathway: Emerging roles of CLC chloride transporters. J Physiol 578:633–640.

Jentsch TJ, Friedrich T, Schriever A, Yamada H. 1999. The CLC chloride channel family. Pflugers Arch 437:783–795.

Komori T. 2006. Regulation of osteoblast differentiation by transcription factors. J Cell Biochem 99:1233–1239.

Kornak U, Kasper D, Bosl MR, Kaiser E, Schweizer M, Schulz A, Friedrich W, Delling G, Jentsch TJ. 2001. Loss of the ClC-7 chloride channel leads to osteopetrosis in mice and man. Cell 104:205–215.

Kubisch C, Schmidt-Rose T, Fontaine B, Bretag AH, Jentsch TJ. 1998. ClC-1 chloride channel mutations in myotonia congenita: Variable penetrance of mutations shifting the voltage dependence. Hum Mol Genet 7:1753–1760.

Lamour V, Detry C, Sanchez C, Henrotin Y, Castronovo V, Bellahcene A. 2007. Runx2- and histone deacetylase 3-mediated repression is relieved in differentiating human osteoblast cells to allow high bone sialoprotein expression. J Biol Chem 282:36240–36249.

Lange PF, Wartosch L, Jentsch TJ, Fuhrmann JC. 2006. ClC-7 requires Ostm1 as a beta-subunit to support bone resorption and lysosomal function. Nature 440:220–223.

Li X, Wang T, Zhao Z, Weinman SA. 2002. The ClC-3 chloride channel promotes acidification of lysosomes in CHO-K1 and Huh-7 cells. Am J Physiol Cell Physiol 282:C1483–C1491.

Livak KJ, Schmittgen TD. 2001. Analysis of relative gene expression data using real-time quantitative PCR and the 2(−Delta Delta C(T)) Method. Methods 25:402–408.

Lyons RM, Keski-Oja J, Moses HL. 1988. Proteolytic activation of latent transforming growth factor-beta from fibroblast-conditioned medium. J Cell Biol 106:1659–1665.

Maki M, Miyazaki H, Nakajima K, Yamane J, Niisato N, Morihara T, Kubo T, Marunaka Y. 2007. Chloride-dependent acceleration of cell cycle via modulation of Rb and cdc2 in osteoblastic cells. Biochem Biophys Res Commun 361:1038–1043.

Nabavi N, Urukova Y, Cardelli M, Aubin JE, Harrison RE. 2008. Lysosome dispersion in osteoblasts accommodates enhanced collagen production during differentiation. J Biol Chem 283:19678–19690.

Nakashima K, Zhou X, Kunkel G, Zhang Z, Deng JM, Behringer RR, de Crombrugghe B. 2002. The novel zinc finger-containing transcription factor osterix is required for osteoblast differentiation and bone formation. Cell 108:17–29.

Okamoto F, Kajiya H, Toh K, Uchida S, Yoshikawa M, Sasaki S, Kido MA, Tanaka T, Okabe K. 2008. Intracellular ClC-3 chloride channels promote bone resorption in vitro through organelle acidification in mouse osteoclasts. Am J Physiol Cell Physiol 294:C693–C701.

Otto F, Thornell AP, Crompton T, Denzel A, Gilmour KC, Rosewell IR, Stamp GW, Beddington RS, Mundlos S, Olsen BR, Selby PB, Owen MJ. 1997. Cbfa1, a candidate gene for cleidocranial dysplasia syndrome, is essential for osteoblast differentiation and bone development. Cell 89:765–771.

Picollo A, Pusch M. 2005. Chloride/proton antiporter activity of mammalian CLC proteins ClC-4 and ClC-5. Nature 436:420–423.

Piwon N, Gunther W, Schwake M, Bosl MR, Jentsch TJ. 2000. ClC-5 Cl— channel disruption impairs endocytosis in a mouse model for Dent's disease. Nature 408:369–373.

Quarles LD, Yohay DA, Lever LW, Caton R, Wenstrup RJ. 1992. Distinct proliferative and differentiated stages of murine MC3T3-E1 cells in culture: An in vitro model of osteoblast development. J Bone Miner Res 7:683–692.

Scheel O, Zdebik AA, Lourdel S, Jentsch TJ. 2005. Voltage-dependent electrogenic chloride/proton exchange by endosomal CLC proteins. Nature 436:424–427.

Simon DB, Bindra RS, Mansfield TA, Nelson-Williams C, Mendonca E, Stone R, Schurman S, Nayir A, Alpay H, Bakkaloglu A, Rodriguez-Soriano J, Morales JM, Sanjad SA, Taylor CM, Pilz D, Brem A, Trachtman H, Griswold W, Richard GA, John E, Lifton RP. 1997. Mutations in the chloride channel gene, CLCNKB, cause Bartter's syndrome type III. Nat Genet 17: 171–178.

Stobrawa SM, Breiderhoff T, Takamori S, Engel D, Schweizer M, Zdebik AA, Bosl MR, Ruether K, Jahn H, Draguhn A, Jahn R, Jentsch TJ. 2001. Disruption of ClC-3, a chloride channel expressed on synaptic vesicles, leads to a loss of the hippocampus. Neuron 29:185–196.

Tang YB, Liu YJ, Zhou JG, Wang GL, Qiu QY, Guan YY. 2008. Silence of ClC-3 chloride channel inhibits cell proliferation and the cell cycle via G/S phase arrest in rat basilar arterial smooth muscle cells. Cell Prolif 41:775–785.

Tu Q, Valverde P, Chen J. 2006. Osterix enhances proliferation and osteogenic potential of bone marrow stromal cells. Biochem Biophys Res Commun 341:1257–1265.

Yang JY, Jung JY, Cho SW, Choi HJ, Kim SW, Kim SY, Kim HJ, Jang CH, Lee MG, Han J, Shin CS. 2009. Chloride intracellular channel 1 regulates osteoblast differentiation. Bone 45:1175–1185.

Yin Z, Tong Y, Zhu H, Watsky MA. 2008. ClC-3 is required for LPA-activated Cl- current activity and fibroblast-to-myofibroblast differentiation. Am J Physiol Cell Physiol 294:C535–C542.

Yoshikawa M, Uchida S, Ezaki J, Rai T, Hayama A, Kobayashi K, Kida Y, Noda M, Koike M, Uchiyama Y, Marumo F, Kominami E, Sasaki S. 2002. CLC-3 deficiency leads to phenotypes similar to human neuronal ceroid lipofuscinosis. Genes Cells 7:597–605.